ELSEVIER

Polymer 41 (2000) 6765–6771

polymer

Polypropylene-*block*-poly(ethylene-*co*-propylene) addition to polypropylene/poly(ethylene-*co*-propylene) blends: morphology and mechanical properties

K. Nitta[a,*], T. Kawada[a], M. Yamahiro[b], H. Mori[b], M. Terano[b]

[a]*Center for New Materials, Japan Advanced Institute of Science and Technology, 1-1 Asahidai, Tatsunokuchi, Ishikawa 923-1292, Japan*
[b]*School of Materials Science, Japan Advanced Institute of Science and Technology, 1-1 Asahidai, Tatsunokuchi, Ishikawa 923-1292, Japan*

Received 19 November 1998; received in revised form 14 June 1999; accepted 24 November 1999

Abstract

The additive effects of a diblock copolymer of polypropylene and ethylene–propylene rubber PP-*b*-EPR(50–50) on the morphology and mechanical properties of PP/EPR(50/50) blends were investigated. It was found from an electron microscopy study that the block copolymer is compatible with the PP phase but incompatible with the EPR phase. Dynamic mechanical spectra showed that the PP-*b*-EPR block copolymers are incorporated into the PP phase, and consequently, the EPR portions of the block are trapped into the interlamellae of PP.

Keywords: Polypropylene; Ethylene–propylene random copolymer; Rheo-optics

1. Introduction

Much attention has been paid to blends of isotactic polypropylene (PP) and olefin elastomers such as ethylene–propylene random block copolymer (EPR) for the sake of both scientific interest and commercial utility in the past two decades [1]. PP/EPR blends have been investigated with the aim of improving impact behavior. A lot of effort is still being made to further improve the mechanical properties and morphology of these blends and to expand their applicability. In such circumstances, the additive effect of a third polymer such as diblock copolymers of PP and EPR (PP-*b*-EPR) is of very scientific and practical interest [2,3].

We have succeeded in synthesizing a complete diblock copolymer of PP and EPR (PP-*b*-EPR) with a short-period polymerization technique [4,5]. It is well-known that the short-period (or stopped-flow) polymerization makes it possible to perform "quasi-living polymerization" during a very short period (up to about 0.2 s) in such a way as to avoid a chain transfer reaction [6,7]. In the previous articles [4,5,8], the block formation of the PP-*b*-EPR copolymer was thoroughly examined using differential scanning calorimetry (DSC), ^{13}C NMR, gel permeation chromatography (GPC), optical microscopy, and cross fractionation chromatography (CFC).

The present work deals with the changes in morphology and dynamic mechanical spectrum of PP/EPR binary blends on the addition of a PP-*b*-EPR block copolymer as well as their effects on tensile mechanical properties.

2. Experimental

2.1. Materials and blend preparation

Two commercial grades of isotactic polypropylene (hPP and rPP) and also a commercial grade of ethylene–propylene rubber (EPR) supplied by TOSOH Corp. were used in this study. The hPP is a homopolymer and rPP is a random block copolymer with 3.2 wt% ethylene. The diblock copolymers of PP and EPR (PP-*b*-EPR) were synthesized by a short-period polymerization method with a $MgCl_2$-supported Ziegler catalyst in toluene at 303 K. The block composition of PP-*b*-EPR was controlled by changing the polymerization times. In this work, the additive effects of a block copolymer PP-*b*-EPR(50–50), in which the numerals represent the weight fraction in percentage of the PP and EPR parts, were investigated. For comparison, the PP-*b*-EPR(75–25) block was used only for some measurements

* Corresponding author. Tel.: + 81-761-51-1621; fax: + 81-761-1625.
E-mail address: nitta@jaist.ac.jp (K. Nitta).

0032-3861/00/$ - see front matter
PII: S0032-3861(99)00895-2

Table 1
Characterization of polymers

Polymers	Composition (%)		$M_w \times 10^{-4}$[a]	M_w/M_n[a]	Ethylene[b] content (mol%)	T_m[c] (K)	Density (kg m^{-3})	Crystal form[d]
	PP	EPR						
hPP	100	0	26	5.7	–	438	909	Monoclini
rPP	100	0	25	6.0	5.4	421	900	Monoclinic
EPR	0	100	11	1.7	63	–	853	–
PP-*b*-EPR(75–25)	75	25	5.1	3.2	17	434	899	Monoclinic
PP-*b*-EPR(50–50)	50	50	4.2	3.0	26	433	892	Monoclinic

[a] Determined by gel permeation chromatography, PP standard.
[b] Determinied by ^{13}C NMR.
[c] Melting temperature determined by DSC.
[d] Determined by wide angle X-ray diffraction.

of dynamic mechanical properties. Details of the polymerization procedure were shown in the previous paper [4]. Their molecular characteristics are summarized in Table 1. The molecular weight and its distribution were determined using a high temperature GPC instrument (Senshu SSC-7100) with *o*-dichlorobenzene as a solvent at 313 K. The ethylene content in the samples was determined by ^{13}C NMR spectra using a Varian Gemini-300 spectrometer.

Various blend polymers such as binary PP/EPR and ternary PP/EPR/PP-*b*-EPR blends were prepared in a solution of xylene at 413 K. The blend polymers were precipitated from the solution into methyl alcohol and then dried in a vacuum oven at 333 K and for 10 h.

2.2. Sample preparation and characterization

The samples were melt pressed in a laboratory hot press at 463 K and at 12 MPa. The film specimens were prepared by quenching from the melts into an ice-water bath. The results of the film characterization were also included in Table 1.

DSC measurements were carried out using a Mettler Tredo calorimeter DSC820 that was calibrated for temperature and melting enthalpy using indium as a standard. The samples of about 10 mg weight sealed in aluminum pans were used for the measurements. The samples were heated from 170 to 500 K at a scanning rate of 10 K/min under a nitrogen atmosphere.

The crystal form of the films was examined by wide-angle X ray diffraction (WAXD). The measurements were carried out with at a scanning speed of 1°/min over a 2θ range from 8 to 40° using a WAXD instrument (Rigaku RINT-2000).

Densities of the films were determined by a floatation method. The binary medium prepared from various ratios of distilled water and ethyl alcohol was used.

2.3. Measurements

The overall morphology of the blend films was examined with a transmission electron microscope model HITACHI H-7100. The ultrathin films were sectioned into slices of 100 nm thickness with an ultramicrotome (Reichert-Nissei ULTRACUTS) at 133 K. It should be noted that the molecular weight of PP-*b*-EPR is much smaller than that of these commercial PPs and EPR polymers. The ultrathin films were then stained with ruthenium tetraoxide for 12 to 24 h. Photographic contrast is produced by selective electron scattering from the stained non-crystalline phase.

The measurements of the linear dynamic mechanical properties were made using a dynamic mechanical analyzer (Rheology DVE-V4) on film specimens of the following dimensions: length 20 mm, width 5 mm, and thickness 0.3 mm. The dynamic tensile moduli, the storage modulus E', the loss modulus E'', and the loss tangent tan $\delta(= E''/E')$ were measured between 120 and 430 K at a constant frequency of 10 Hz and a heating rate of 2 K/min.

Stress–strain behavior in the uniaxial tension was measured using a Shimadzu AGS-5 kN. The sample specimens were cut with a dumbbell shape in which the gauge length is 10 mm. The tensile strain was calculated from the ratio of the increment of the length between clamps to the initial gauge length. The tensile stress was determined by dividing the tensile load by the initial cross section. The stress–strain curves at 298 K were measured at a constant cross-head speed of 5, 10, 20, and 50 mm/min. The tensile strain was calculated from the ratio of the increment of the length between clamps to the initial gauge length.

In order to examine the orientation behavior of PP crystals (*c*-axis) for the present samples, we measured the infrared dichroism of the 998 cm^{-1} band simultaneously with the tensile load during elongation. Details of these experimental procedures were presented in the previous study [9]. Here, we briefly repeat the main outlines.

A tensile tester was placed in a Fourier-transform infrared (FTIR) spectrometer (JASCO FT-IR500) in such a way as to allow the infrared beam to pass a central point on the film mounted on the tensile tester.

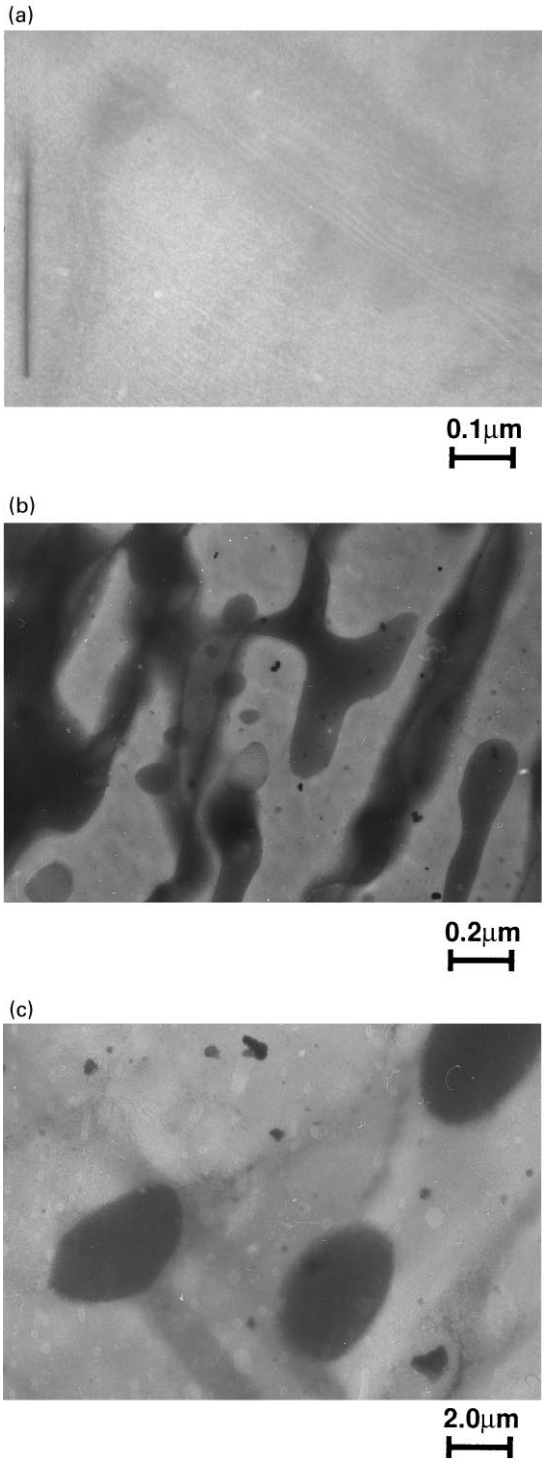

Fig. 1. TEM micrographs of thin sections for (a) PP-*b*-EPR(50–50) diblock; (b) rPP/EPR(50/50) blend; and (c) the addition of 20 wt% of PP-*b*-EPR(50–50) to rPP/EPR(50/50) blend.

The tensile tester was designed with upper and lower clamps to symmetrically move from the central point or the beam point on the film. The cross-head speed was 1 mm/min in all cases.

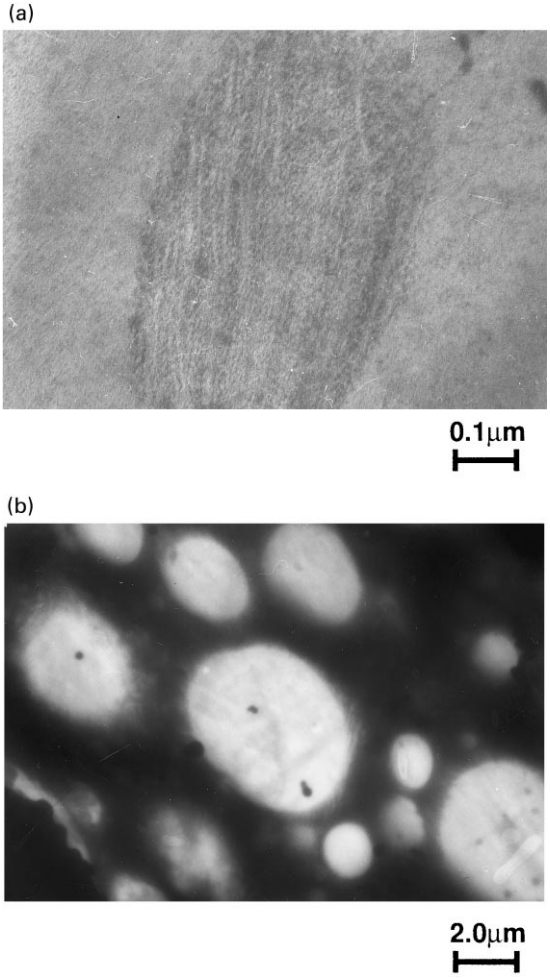

Fig. 2. TEM micrographs of thin sections for (a) the addition of 20 wt% of PP-*b*-EPR(50–50) to hPP homopolymer; (b) the addition of 20 wt% of PP-*b*-EPR(50–50) to EPR copolymer.

3. Results and discussion

3.1. Morphology

TEM micrographs for the typical film specimens are exemplified in Figs. 1 and 2, in which the dark regions correspond to the stained EPR rich phase, whereas bright regions correspond to the crystalline PP rich phase. The PP-*b*-EPR(50–50) block film exhibits a homogeneous morphology (Fig. 1a), whereas the rPP/EPR(50/50) blend exhibits a bicontinuous phase separation (Fig. 1b). The TEM micrographs of the rPP/EPR blends were very similar to those of the hPP/EPR blends. As shown in Fig. 1c, the addition of 20 wt% of PP-*b*-EPR(50–50) into the binary rPP/EPR(50/50) blend causes a change in domain size of EPR, in which the EPR phase appears to be completely surrounded by the PP phase, although the content of EPR in the blends does not change with the addition of PP-*b*-EPR. Based on the fact that the PP phase was enlarged, one may infer that the majority of the PP-*b*-EPR is embedded in the PP phase.

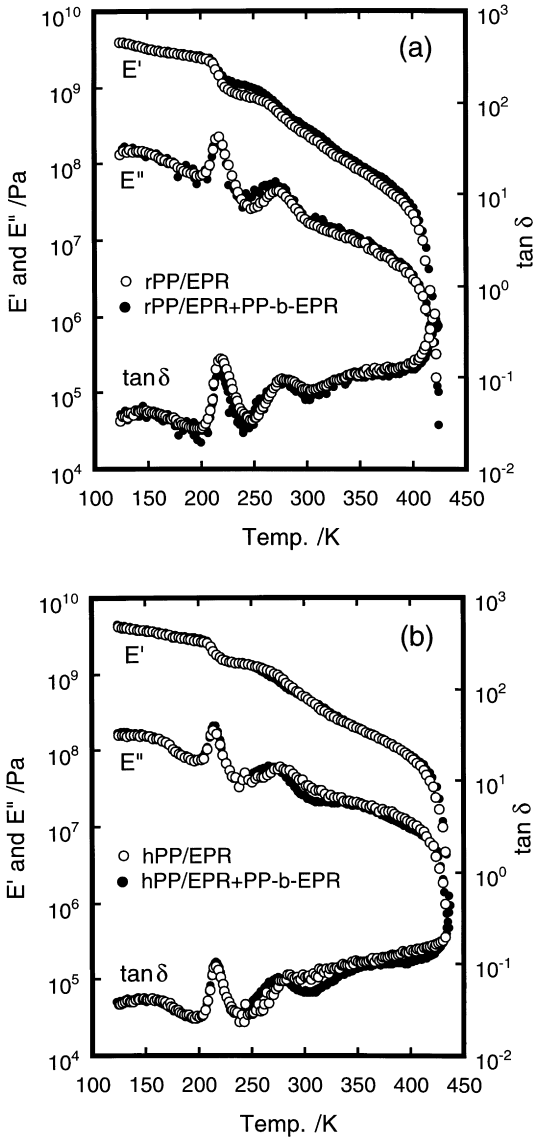

Fig. 3. Temperature dependence of the mechanical storage modulus (E'), loss modulus (E'') and loss tangent (tan δ) with temperature for (a) rPP/EPR(50/50) blend and the addition of 20 wt% of PP-*b*-EPR(50–50) to rPP/EPR(50/50); and (b) hPP/EPR(50/50) blend and the addition of 20 wt% of PP-*b*-EPR(50–50) to hPP/EPR(50/50).

Fig. 2 compares the morphological features of 50 wt% addition of the PP-*b*-EPR to the hPP and EPR polymers. The morphology of the blend with EPR is clearly different from that of the blend with PP. The PP/PP-*b*-EPR exhibits a homogeneous, morphology whereas the PP domains are dispersed into the EPR matrix in the EPR/PP-*b*-EPR sample. This suggests that the PP-*b*-EPR block copolymer is compatible with PP but incompatible with EPR.

3.2. Dynamic mechanical properties

Fig. 3a and b show the effects of 20 wt% addition of the PP-*b*-EPR(50–50) block on the dynamic mechanical behavior of the PP/EPR(50/50) blends. In these figures, temperature dependences of E'' in the glass-relaxation region are shown. As seen in these figures, the higher temperature peak is ascribed to the T_g of the amorphous region of PP, and the lower relaxation peak is to the T_g of the EPR component. It was found that the T_g of PP is shifted to a lower temperature on adding PP-*b*-EPR, whereas the T_g of the EPR component does not change with the addition of PP-*b*-EPR. Fig. 4 summarizes the additive effect of PP-*b*-EPR(50–50) on the two T_gs of PP/EPR(50/50) blends. This strongly suggests that the PP-*b*-EPR molecules are incorporated into PP phase, resulting in trapping the EPR portions of the PP-*b*-EPR into the interlamellar regions of PP. The

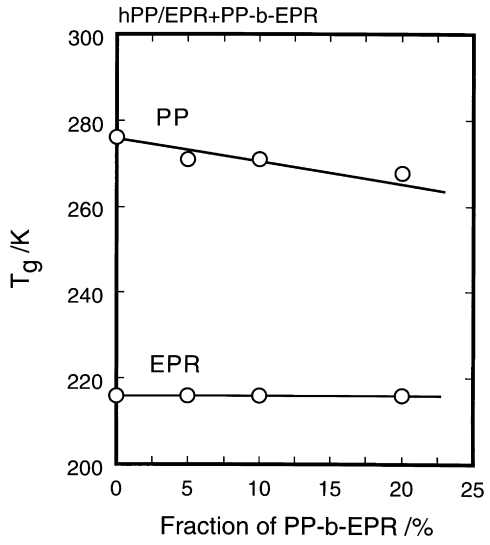

Fig. 4. Compositional dependence of the glass transition temperatures of PP and EPR for the addition of PP-*b*-EPR(50–50) to PP/EPR(50/50) blend.

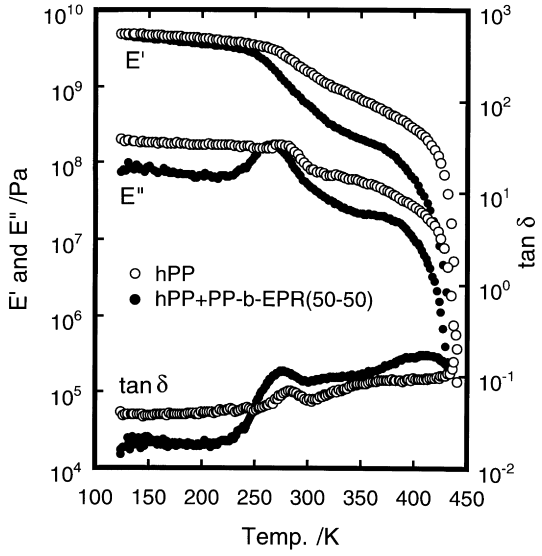

Fig. 5. Temperature dependence of the mechanical storage modulus (E'), loss modulus (E'') and loss tangent (tan δ) with temperature for (○) hPP and (●) binary (50/50) blend of hPP and PP-*b*-EPR(50–50).

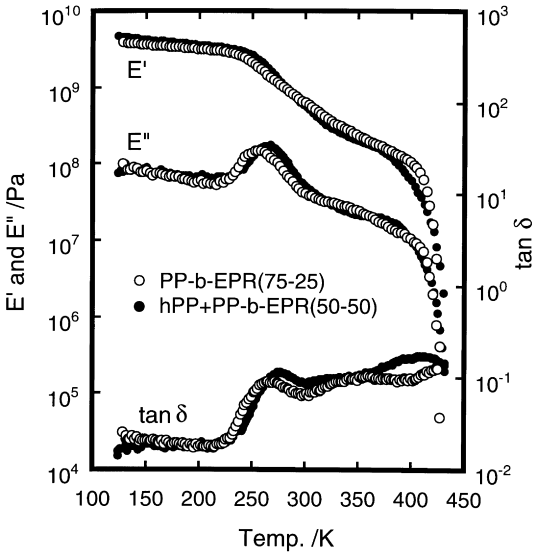

Fig. 6. Temperature dependence of the mechanical storage modulus (E'), loss modulus (E'') and loss tangent (tan δ) with temperature for (○) PP-*b*-EPR(75–25) diblock and (●) binary (50/50) blend of hPP and PP-*b*-EPR(50–50).

morphological features in the TEM observation are in agreement with the dynamic mechanical behavior of the PP/EPR/PP-*b*-EPR ternary blends.

The addition of an amount (50 wt%) of PP-*b*-EPR(50–50) to the PP homopolymer affects the dynamic mechanical spectra. As shown in Fig. 5, the mechanical loss peak corresponding to T_g in the PP/PP-*b*-EPR(50/50) blend is broadened and shifted down in temperature relative to that of the PP homopolymer. This result also suggests that the EPR

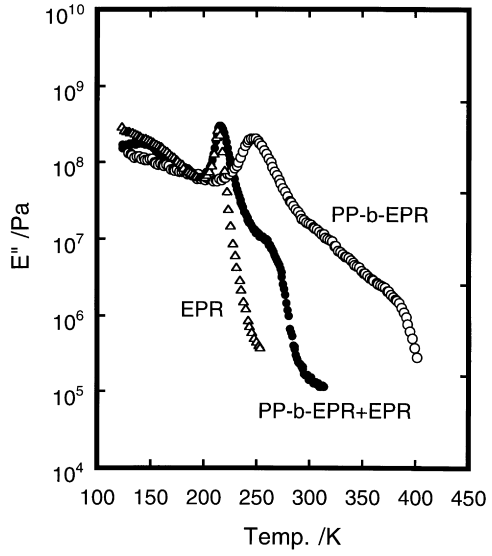

Fig. 7. Temperature dependence of the mechanical storage modulus (E'), loss modulus (E'') and loss tangent (tan δ) with temperature for (△) EPR, (○) PP-*b*-EPR(50–50) diblock, and (●) binary (50/50) blend of EPR and PP-*b*-EPR(50–50).

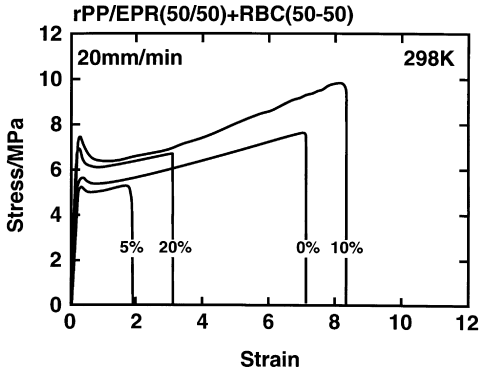

Fig. 8. Additive effect of PP-*b*-EPR(50–50) to hPP/EPR(50/50) blend on stress–strain behavior at 298 K and 20 mm/min.

component is trapped in the amorphous region of PP consistent with the finding that the PP/PP-*b*-EPR blend shows no phase separation in the TEM micrograph (see Fig. 2a). Also, the addition of PP-*b*-EPR to PP causes a reduction in the dynamic moduli of PP over the entire temperature range. Fig. 6 compares the dynamic mechanical spectra of a PP-*b*-EPR(75–25) block sample containing the same EPR content with the PP/PP-*b*-EPR(50/50) blend. The overall spectrum of PP/PP-*b*-EPR is found to be almost the same as that of its corresponding block copolymer, although the PP-*b*-EPR(75–25) block sample manifests a slightly lower T_g.

Fig. 7 shows the effect of adding 50 wt% of the PP-*b*-EPR(50–50) block into the EPR copolymer on the dynamic mechanical relaxation process. For comparison, the dynamic mechanical spectrum of PP-*b*-EPR(50–50) is included in the figure. As shown in Fig. 7, the EPR/PP-*b*-EPR blend shows two dispersion peaks which are located at the T_gs of EPR and PP-*b*-EPR(50–50), suggesting that PP-*b*-EPR is immiscible with EPR. This may be due to the fact that the ethyl content or molecular mass of the EPR portions of PP-*b*-EPR is different from that of EPR. This result is consistent with the finding that the EPR/PP-*b*-EPR blends

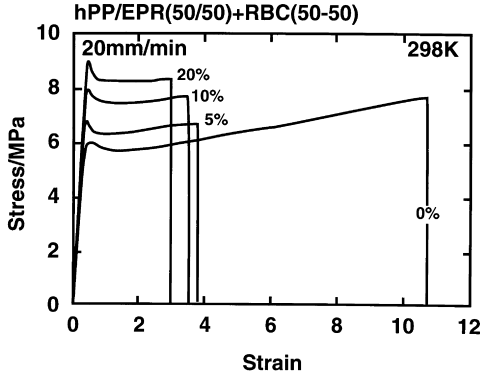

Fig. 9. Additive effect of PP-*b*-EPR(50–50) to rPP/EPR(50/50) blend on stress–strain behavior at 298 K and 20 mm/min.

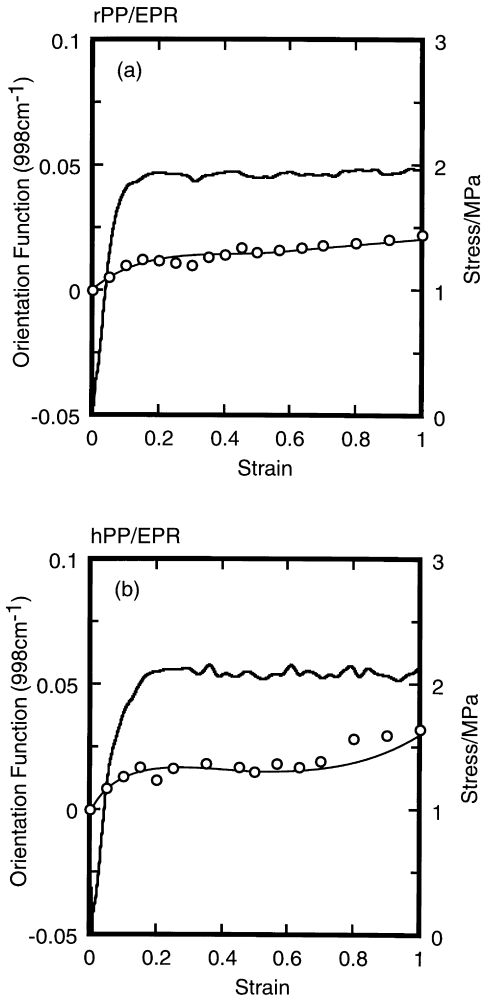

Fig. 10. Strain dependence of orientation function for 998 cm^{-1} band of (a) rPP/EPR(50/50) blend and (b) hPP/EPR(50/50) blend.

shows a phase-separated morphology and that the bright regions are completely surrounded by EPR regions (see Fig. 2b).

3.3. Tensile mechanical properties

The addition of the PP-*b*-EPR(50–50) to PP/EPR(50/50) blends strongly modifies the overall stress–strain behavior as exemplified in Figs. 8 and 9. It was found that the stress or yield stress increases with increasing PP-*b*-EPR content, whereas the addition of the PP-*b*-EPR to hPP/EPR blends causes a drastic reduction in the elongation at break. In the case of rPP/EPR, however, the largest value of elongation at break is found for the blend with 10 wt% PP-*b*-EPR. The similar tendency was confirmed under different elongational conditions.

It was found from the present study that the addition of PP-*b*-EPR induces not only a lowered T_g of PP but also the discontinuity of the EPR phase. The effect of the lowered T_g of PP leads to ductility; on the contrary, the effect of the discontinuity of EPR phases leads to a brittle nature. The superiority of the former effect over the latter effect for such multiphase polymers is sensitive to the structural feature of their components, phase continuity, and morphology conversion. It is indicated that the effect of lowering the T_g of PP is superior to the dispersion effect of EPR in the case of the addition of 10 wt% PP-*b*-EPR to rPP/EPR.

3.4. Deformation mechanism

In order to examine the orientation behavior of PP crystals during tensile deformation, we measured the dichroism ratio of the 998 cm^{-1} band simultaneously with the stress–strain curve. As shown in Fig. 10, the rPP/EPR(50/50) and hPP/EPR(50/50) blends showed no well-defined yield points, and the both blends were elongated without orientation of the PP chains. On the other hand, as shown in Fig. 11, the addition of PP-*b*-EPR copolymer induces orientation of PP chains and this leads to a yield point. This is plausible since the stress concentration occurs on the PP phase because of the discontinuity of the EPR domains.

It is interesting to note that the 20 wt% addition of the PP-*b*-EPR(50–50) to the rPP/EPR(50/50) blends induces orientation of PP, whereas the orientation function of PP crystals for hPP/EPR/PP-*b*-EPR shows a great decrease and then increases after passing a minimum around 50% strain. There is a great difference in the additive effects of PP-*b*-EPR between rPP/EPR and hPP/EPR on the deformation mechanism. This will be due to the fact that the lamellar orientation and rotation forced by the external load causes the chain axis in the PP crystals (*c*-axis) to orient perpendicular to the stretching direction. The further elongation induces the lamellar fragmentation and this can lead to the orientation of the *c*-axis becoming progressively greater with increasing strain. In the case of rPP/EPR/PP-*b*-EPR, the lamellar fragmentation occurs more easily in the rPP lamellae with additional defects due to the comonomer (ethylene) units [10]. Therefore, the orientation function of the *c*-axis increases immediately. Moreover, the difference in the tensile behavior between rPP/EPR/PP-*b*-EPR and hPP/EPR/PP-*b*-EPR, as described in the previous section, may be related to the difference in their deformation mechanisms. More research is necessary to elucidate the negative and positive orientation behaviors of these tertiary blends.

4. Conclusions

The results presented show that the PP-*b*-EPR(50–50) block copolymer is incompatible with the EPR copolymer but compatible with isotactic PP polymers. A homopolymer (hPP) and a random block copolymer with 3.2 wt% ethylene (rPP) exhibited essentially similar compatibility. Thus, it was found that the majority of the PP-*b*-EPR copolymer is incorporated into the PP phase in the PP/EPR blends, and

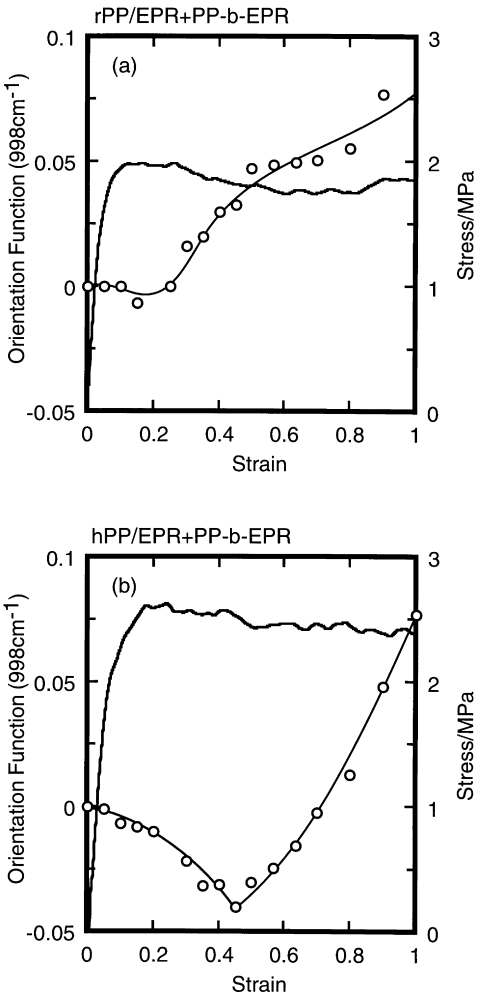

Fig. 11. Strain dependence of orientation function for 998 cm^{-1} band of (a) rPP/EPR/PP-*b*-EPR tertiary blend and (b) hPP/EPR/PP-*b*-EPR tertiary blend, in which the amount (20 wt%) of PP-*b*-EPR(50–50) is added to PP/EPR(50/50) blends.

consequently the EPR portions of the block are trapped into the interlamellar region of PP. As a result, the addition of the PP-*b*-EPR(50–50) block copolymers to the PP/EPR(50/50) blend has an influence on the morphology of the binary blend and the glass transition temperature and moreover, affects their tensile mechanical properties. Although the chemical structure of these copolymers is of an intermediate nature between PP and EPR, they cannot always act as "compatibilizing agents" between the amorphous region of PP and the EPR phase. This means that a better homogenization failed to be achieved with the addition of the PP-*b*-EPR(50–50) block. This may be due to the fact that the PP portions in the PP-*b*-EPR(50–50) block possibly cocrystallized with PP molecules during the melt-crystallization process because the PP-*b*-EPR molecule has the potential to possess a higher mobility resulting from its considerably lower molecular weight compared with pure PP or EPR polymers.

It is of very interest to note that there is a quite difference in the additive effects of PP-*b*-EPR between rPP/EPR and hPP/EPR on the PP crystal orientation process during a elongation. Thus, it was found that the rPP/EPR/PP-*b*-EPR shows the orientation of PP crystals (*c*-axis) in the parallel direction to the elongation, whereas hPP/EPR/PP-*b*-EPR shows the orientation of PP crystals (*c*-axis) in the perpendicular direction. In future, details of molecular mechanism for the orientation behavior of PP crystals will be studied.

References

[1] Martuscelli E. Structure and properties of polypropylene–elastomer blends. In: Karger-Kocsis J, editor. Polypropylene, structure, blends and composites, London: Chapman & Hall, 1995. p. 95–140.
[2] Wang L, Huang B. J Polym Sci, Polym Phys Ed 1991;29:1447.
[3] Lohse DJ, Datta S, Kresge EN. Macromolecules 1991;24:561.
[4] Mori H, Yamahiro M, Tashino K, Ohnishi K, Nitta K, Terano M. Macromol Chem Rapid Commun 1995;16:247.
[5] Yamahiro M, Mori H, Nitta K, Terano M. Macromol Chem Phys 1999;200:134.
[6] Keii T, Terano M, Kimura K, Ishii K. Macromol Chem Rapid Commun 1989;8:203.
[7] Terano M, Kataoka T, Keii T. J Mol Catal 1989;56:203.
[8] Yamahiro M, Mori H, Nitta K, Terano M. Polymer 2000 (in press).
[9] Nitta K, Okamoto K, Yamaguchi M. Polymer 1998;39:53.
[10] Nitta K, Takayanagi M. J Polym Sci, Polym Phys Ed 1999;37:357.